Tailoring the optical parameters of optical fiber interferometer with dedicated boron-doped nanocrystalline diamond thin film

Daria Majchrowicz[*,1], Monika Kosowska[1], Przemysław Struk[2], Małgorzata Jędrzejewska-Szczerska[,1]**

[1] Department of Metrology and Optoelectronics, Faculty of Electronics, Telecommunications and Informatics, Gdańsk University of Technology, Narutowicza Street 11/12, 80-233 Gdańsk, Poland
[2] Department of Optoelectronics, Faculty of Electrical Engineering, Silesian University of Technology, Krzywoustego Street 2, 44-100 Gliwice, Poland

Received ZZZ, revised ZZZ, accepted ZZZ
Published online ZZZ (Dates will be provided by the publisher.)

Keywords boron-doped diamond thin film, optical fiber interferometer, interference

* Corresponding author: e-mail dmajchrowicz@eti.pg.gda.pl, Phone: +48 583 471 361, Fax: +48 583 471 848
** e-mail mjedrzej@eti.pg.gda.pl, Phone: +48 583 471 361, Fax: +48 583 471 848

Optical fiber interferometer using nanocrystalline boron-doped diamond film was investigated. The diamond films were deposited on glass plates using a Microwave Plasma-Enhanced Chemical Vapour Deposition (μPE CVD) system. The growth time was 3h, with boron doping level of 10 000 ppm producing films (B-NCD-10) of thickness ~ 200 nm. The presence of boron atoms in the diamond film is evident in Raman spectrum as peaks at 1212 cm^{-1} and 1306 cm^{-1}. The scanning electron microscopy (SEM) images showed homogenous and continuous surface morphology, thus enabling the use of the diamond film as a reflective layer in fiber optic devices. Optical fiber interferometric sensor in Fabry-Pérot configuration with a diamond reflective layer as a mirror was designed and built. Measurements were performed using two superluminescent diodes with central wavelengths of 1300 μm and 1550 μm. Detection of the measured signal was achieved using an optical spectrum analyzer. All devices were connected with commercially available, single-mode telecommunications fibers and coupler. Using B-NCD-10 films in fiber optic interferometer we obtained very high value of measured signal contrast equal to 0.99. The use of B-NCD-10 film as a reflective surface allows the Fabry-Pérot cavity length to be reduced while achieving very good signal visibility. Consequently, the volume of the sample in the cavity can be reduced, compared with that than those for traditional mirrors.

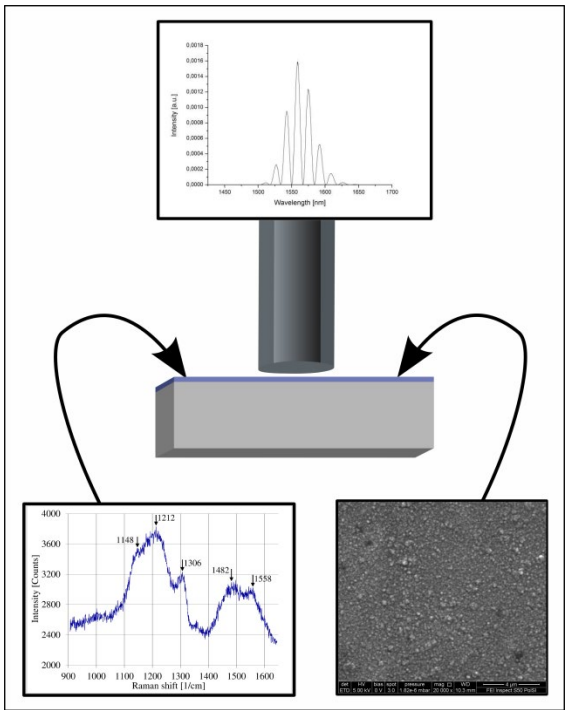

1 Intoduction Optical fiber interferometers are commonly used as sensors in many areas of human life because of their small size, low weight and very good metrological parameters [1–4]. The metrological parameters of optical fiber interferometer (spatial resolution, stability, accuracy)

are determined mainly by the visibility of the measured signal spectrum. On the other hand, the visibility of measurement signal spectrum depends on the quality of the reflecting surfaces. That is why mirrors are so important elements of an optical fiber interferometers.

In traditional construction of interferometers the reflecting surfaces are made from silver. This material has limited resistance to chemicals and it is susceptible to mechanical damage, which limits its use in interferometers which have contact with biochemical materials. Therefore, as we wanted to use our interferometer in a biosensing application, the mirrors must be biocompatible and have sufficient chemical resistance, which necessitates the use of a new material. Such a material should be chemically inert and resistant to mechanical damage. Thin diamond films are appreciated due to high hardness, chemical stability and biocompatibility [5–7]. They have a low coefficient of thermal expansion and a high thermal conductivity. Additionally, they are chemically inert and immune to abrasion [8]. Thanks to the aforementioned properties, they can be used in sensing optical fiber interferometers as reflection layers, or mirrors. Boron-doped thin diamond films increase chemical stability of such interferometers and modifies their electrical properties [9]. The smaller size of crystallites in the boron-doped films improves their optical properties such as reflectivity [10,11]. The use of such films in the interferometric sensor allows for simultaneous measurements by optical and electrochemical methods.

Boron-doped diamond films are widely used in electrochemistry due to their electronic properties and chemical stability [12], while being a promising material for biological or organic sensors [13,14]. Moreover, these films are used as materials for electrodes for mineralization of hazardous organic compounds [12]. Due to their biocompatibility, these films are an excellent material to detect various types of proteins or DNA [15]. Thin diamond films are mainly synthesized using microwave plasma-enhanced chemical vapor deposition (μPE CVD). Using this process, it is possible to deposit films whose key properties, such as thickness, texture, grain size, chemical composition, defect concentration and surface morphology, can be modified [16] by adjusting process parameters.

Our previous research described by D. Milewska et. al. (2016) [3, 4] was focused on the possibility of using thin diamond films in fiber optic sensors. In these articles [3,4] undoped and boron-doped diamond films were investigated. The films were deposited on glass plates and silicon substrates and the growth time was 90 and 270 minutes. Thanks to these studies we have been able to determine which parameters have a significant influence on the optical parameters of diamond films.

Recently, we presented a boron-doped diamond thin film synthesised by μPE CVD with a growth time of 180 minutes. Additionally, hydrogenation was applied prior to diamond deposition and cone-shaped holder was used.

In this paper, we show a Fabry-Pérot interferometer with B-NCD-10 film acting as a mirror, with cavity length of 60 μm, as previously not reported in the literature known to us. The construction was obtained by tailoring deposition parameters. The production process of diamond film was enhanced with two additional elements: hydrogenation and use of a cone-shaped holder.

The use of hydrogenation influenced the quality of the glass substrate and improved the homogeneity of the diamond films that were deposited on these surfaces. Growth of the diamond film on the cone-shaped holder causes a decrease in crystallite size. The doping of boron also influences the reduction of crystallites. The use of hydrogenation, cone-shaped holder and doping of boron significantly influenced the layer parameters.

2 Materials and methods

2.1 Nanocrystalline diamond film growth The boron-doped diamond films elaborated for the research described in this article were deposited on glass plates (10 × 10 mm; 1 mm thick). Before deposition of nanocrystaline diamond the substrates were prepared in a three-step process: cleaning, hydrogenation, and sonication, detailed by *M. Ficek . et. al. (2016)* [16].

The boron-doped diamond film was grown on cone-shaped holder [17,18]. The doping level of boron in the gas phase was 10 000 ppm using diborane (B_2H_6) dopant precursor. The molar ratio of CH_4-H_2 mixture was kept at 1% of gas volume of total flow rate (300 sccm). The process pressure was kept at 50 Torr and the substrate temperature was estimated at 500 °C. The microwave plasma power for synthesis of boron-doped diamond was maintained at 1300 W. The excited plasma was ignited by microwave radiation (2.45 GHz) [19,20]. The deposition time was 180 min. The thin boron-doped diamond films had their thickness in the range of 200 nm.

2.2 B-NCD-10 films surface and structure investigation

2.2.1 SEM images of diamond film The first step of the research was focused on the investigation of the surface topography as well as surface roughness of the boron-doped diamond films. The research of the surface topography was carried out with the use of two complementary methods: scanning electron microscopy - SEM and atomic force microscopy - AFM. The investigation of the surface topography of a diamond film on a relatively large surface area ~15 x 15 μm was carried out by SEM method (Inspect S50, FEI company, USA) with magnification x20 000. The resulting SEM image presented in Figure 1 shows that the surface of the diamond film is in the form of crystallites with size in the range of ~0.1-0.45 μm. The film is continuous and homogenous with no cracks. Therefore, this film can act as a reflective layer in an optical fiber interferometer.

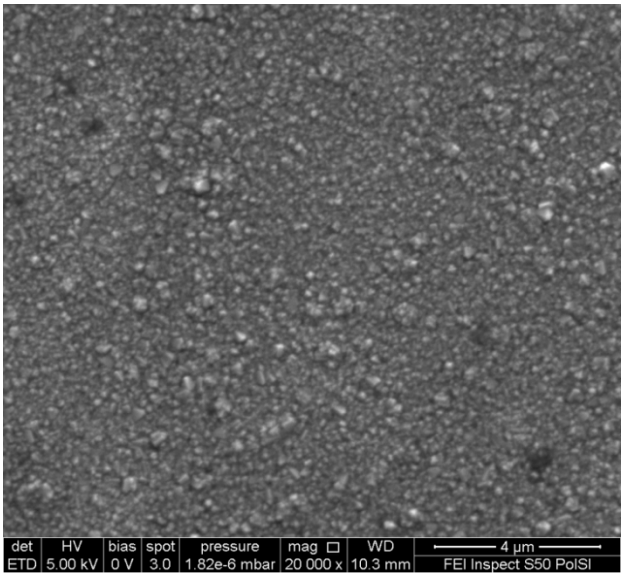

Figure 1 The SEM image of the surface topography of the boron-doped diamond film (B-NCD-10)

2.2.2 AFM images of diamond film The second step of the research on boron-doped diamond film surface properties was focused on the determination the surface roughness. The scanning of diamond film surfaces was conducted by using AFM (NT-MDT company, Russia) with a HA_NC probe. The AFM probe worked in a semi-contact mode, with resonant frequency f_R = 140 kHz and scanning frequency fs = 0.25 Hz. The 3D surface morphology of the investigated film is presented in Figure 2. The root mean square roughness R_q of tested films was calculated in Nova software (NT-MDT company) based on equation (1) [21]. The boron doping of the diamond film increase the Rq values in comparison to undoped diamond film. The Rq of undoped diamond film was equal to 13 nm, while the Rq of boron-doped diamond film was equal to 22.1 nm. Both Rq values are acceptable for use of these films as mirrors in Fabry-Pérot interferometers.

$$R_q = \sqrt{\frac{1}{N_x \cdot N_y} \sum_{j=1}^{N_y} \sum_{i=1}^{N_x} \left(Z_{ij} - \mu\right)^2} \tag{1}$$

where: N_x, N_y – is the number of points on X, Y axis, $Z_{ij}=Z(X_i, Y_j)$ is a discrete function, μ - average (mean height) [21].

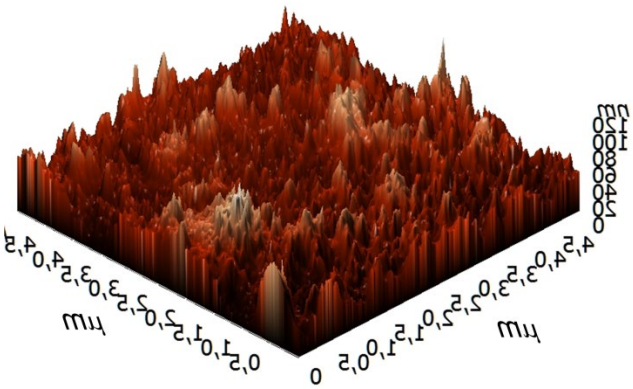

Figure 2 AFM image of 5 × 5 µm areas of B-NCD – 10 film deposited on glass substrates.

2.2.3 Raman Spectra of diamond film The Raman spectra of investigated diamond films were measured by the N-TEGRA Spectra (NT-MDT Company, Russia) measurement setup. During the research the tested sample was illuminated by a laser with the central wavelength λ = 532 nm. The Raman spectrum of a boron-doped diamond film (B-NCD-10) deposited on a glass plate is presented in Figure 3. The spectrum represents a typical signal signatures for the boron-doped diamond film. The Raman peak for 1148 cm^{-1} may be associated with nanocrystalline diamond as well as tetrahedral amorphous carbon (ta-C) with ~ 90% sp^3 bonding, the Raman peak for 1482 cm^{-1} (D band) can be caused by the amorphous carbon phase sp^2 as well as sp^3, the Raman peak for 1558 cm^{-1} (G band) can be caused by sp^2 bonded amorphous carbon [22]. The doping of the diamond film by boron atoms is visible in Raman spectrum as peaks for 1212 cm^{-1} as well as for 1306 cm^{-1} [22–24]. For comparison the Raman spectrum of a undoped diamond film deposited on a glass plate is presented in Figure 4, the spectrum has no characteristic peak for 1212 $1/cm^{-1}$ which is visible for boron doped diamond film.

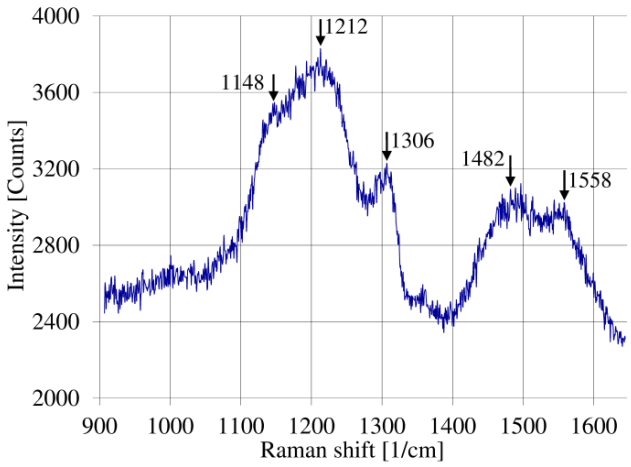

Figure 3 The Raman shift of the boron-doped diamond film deposited on a glass plate.

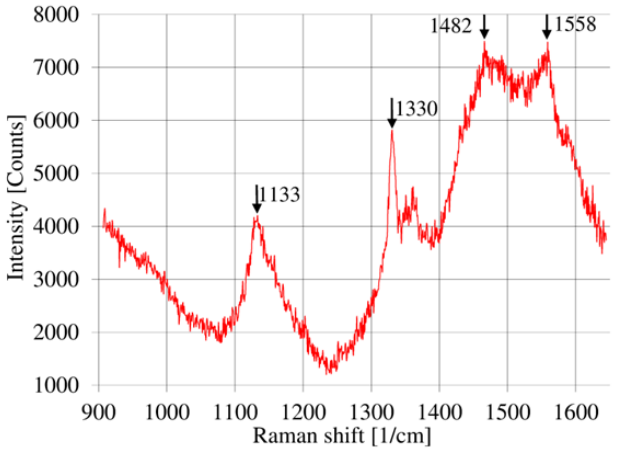

Figure 4 The Raman shift of the undoped diamond film deposited on a glass plate.

2.3 Experiment set-up To investigate the performance of a B-NCD-10 film in a fiber optic interferometer the experimental set-up, shown in Figure 5, was built. It consists of a light source, fiber optic coupler, optical fiber links, optical spectrum analyzer and the measurement head. Two superluminescent diodes (SLED, Superlum Ltd., Ireland) type S-1550-G-I-20, with the central wavelength $\lambda = 1550$ nm, the spectrum width $\Delta\lambda_{FWHM} = 45$ nm and type S1300-G-I-20 with the central wavelength $\lambda = 1290$ nm, the spectrum width $\Delta\lambda_{FWHM} = 50$ nm were applied as broadband sources.

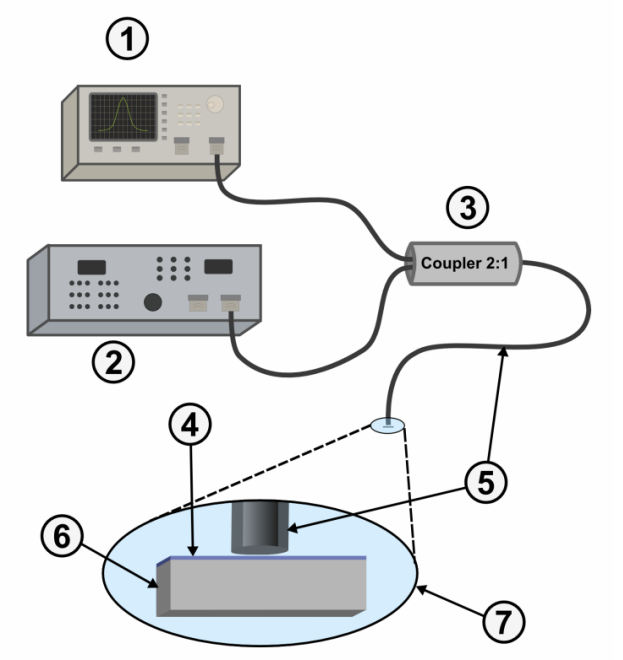

Figure 5 Experimental set-up: 1) optical spectrum analyzer, 2) source 3) fiber optic coupler, 4) B-NCD-10 thin film 5) optical fiber link , 6) glass plate, 7) sensing interferometer.

The measurement head was built as a fiber optic Fabry-Pérot interferometer working in reflective mode. The first mirror of the interferometer was made by the boundary fiber tip/air and the second by the boundary air/B-NCD-10 film (Figure 6). The interferometer was built in such a way that its spectral reflectance was similar to that of a two beam interferometer. Therefore, optical signal reflected from the first and the second mirror interfered with each other and were detected using an optical spectrum analyzer (AQ6319, Ando, Japan). Devices were connected to a commercially available 50:50 coupler made from single-mode optical fiber (SMF-28, Thorlabs, USA).

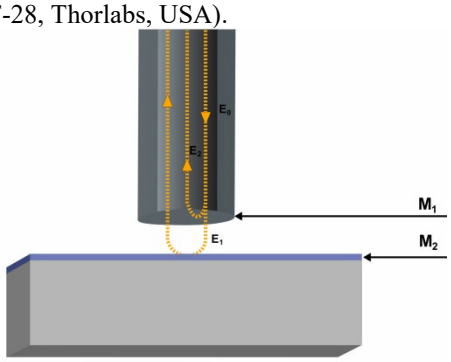

Figure 6 Extrinsic Fabry-Pérot interferometer working in reflective mode: M_1, M_2 – mirrors, E_0 – the amplitude of an electric vector of an incident wave; E_1, E_2 – the amplitude of an electric vector of wave reflected of the first and second mirror, respectively.

3 Results The measurements of the optical signal from the Fabry-Pérot interferometer with B-NCD-10 as a reflective layer were performed with the two super luminescent sources. The influence of the cavity length of the interferometer on the visibility of the measured signal was investigated.

The visibility (V) value of spectral contrast in the spectrum of measured signal was calculated by formula [25,26]:

$$V = \frac{I_{max} - I_{min}}{I_{max} + I_{min}} \tag{2}$$

where: I_{max} – maximum intensity of the measured signal, I_{min} – minimum intensity of the central measured signal. During each series of measurements we changed the cavity length from 0 to 200 µm with increment of 20 µm. The visibility value for two sources with different central wavelengths (1290 nm and 1550 nm) are shown in Table 1.

Table 1 The value of visibility of the measured signal for different light sources (1290 nm and 1550 nm).

Cavity length [µm]	The value of visibility for light source 1290 nm	The value of visibility for light source 1550 nm
20	0.93	0.89
40	0.98	0.97
60	0.99	0.99
80	0.98	0.99
100	0.93	0.96
120	0.88	0.93
140	0.81	0.89
160	0.76	0.83
180	0.70	0.79
200	0.65	0.74

As it can be noted from Table 1, the use of B-NCD-10 film as reflective surfaces allows us to achieve high visibility values. The optimal (i.e. the highest) visibility value was observed for the cavity length of 60 µm. In Figure 7, we present spectra recorded with the 1290 nm source and the cavity length of 60, 120, 160 and 200 µm.

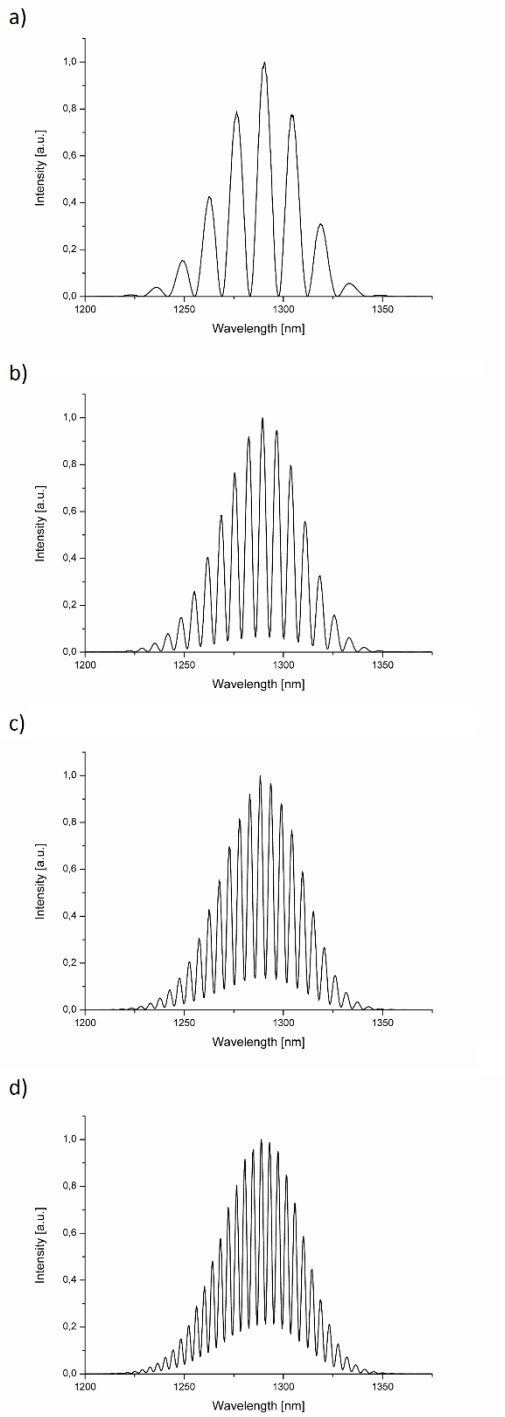

Figure 7 Measurement signal from the interferometer with the 1290 nm source. The length of Fabry–Pérot cavity is: a) 60 µm, b) 120 µm, c) 160 µm, d) 200 µm.

In Figure 8, we present spectra recorded with the 1550 nm source and the cavity length of 20, 80, 140 and 200 µm.

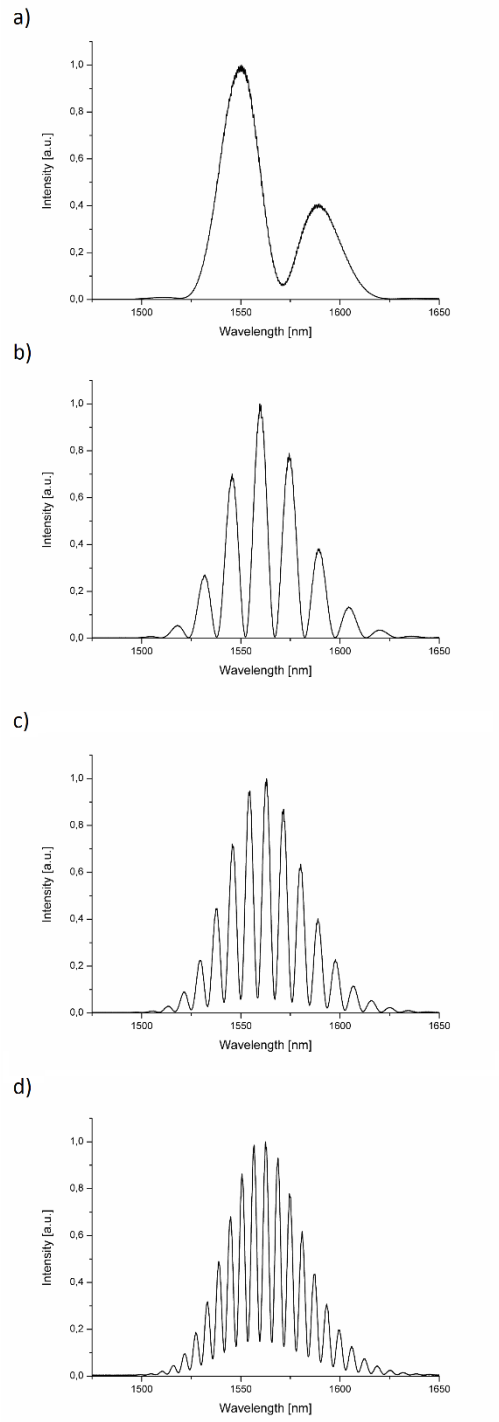

Figure 8 Measurement signal from the interferometer with the 1550 nm source. The length of Fabry–Pérot cavity is: a) 20 μm, b) 80 μm, c) 140 μm, d) 200 μm.

The measured signal obtained from interferometer with undoped and boron-doped diamond film is shown in Figures 9 and 10. Representative spectra for cavity length 60 μm and 80 μm are presented. The use of boron-doped diamond film increases visibility value by 8,6% relative to undoped diamond film for the 1290 nm light source and by 14% for the 1550 nm light source.

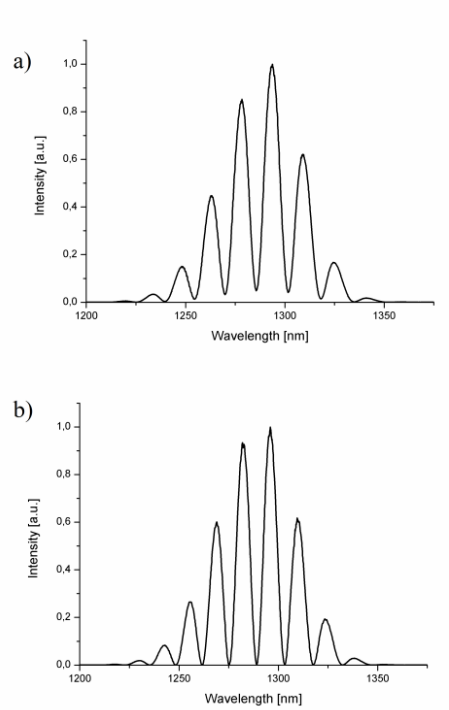

Figure 9 Measurement signal from interferometer with: a) the undoped diamond film, b) the boron-doped diamond film. The 1290 nm light source was used. The length of Fabry–Pérot cavity was 60 μm.

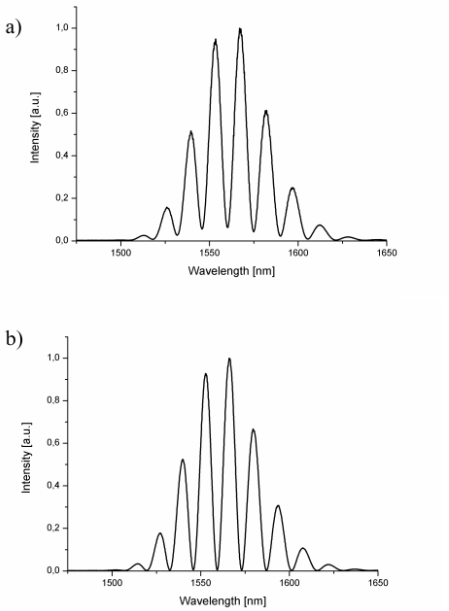

Figure 10 Measurement signal from interferometer with: a) the undoped diamond film, b) the boron-doped diamond film. The 1550 nm light source was used. The length of Fabry–Pérot cavity is 80 μm.

4 Conclusion In this paper we have shown that we are able to tailor the optical parameters of optical fiber interferometer by the use of the dedicated boron-doped nanocrystalline diamond thin film. The use of a Fabry-Pérot interferometer with boron-doped diamond film allows the measurement of very small samples of investigated liquids to be made. This is possible thanks to cavity length of about 60 µm, which we can construct because of using B-NCD-10 film as the mirror. The visibility of the signal measured in our interferometer achieved very high value equal to 0.99, which confirms usefulness of boron-doped diamond film in optical fiber interferometer.

Therefore, the use of B-NCD-10 film as the reflective surface allows very good visibility of the signal to be achieved for much smaller cavity length than that for conventional mirrors [4]. This property can be successfully used to study very small samples such as: clinical bio-fluids, hazardous chemicals, etc. As a result, it occurs that researches on utilization of this material, with systems in low-coherent optical fiber interferometers, is interesting for both the basic and applied research point of view.

Acknowledgements This study was partially financed by the DS Programs of the Faculty of Electronics, Telecommunications and Informatics of the Gdańsk University of Technology as well as by the grant "Research of Young Scientists - BNM/563/RE4/2016" financed by the Faculty of Electrical Engineering, Silesian University of Technology Poland. Authors would like to thank Mr. Mateusz Ficek for providing the diamond thin films.

References

1. M. Hirsch, D. Majchrowicz, P. Wierzba, M. Weber, M. Bechelany and M. Jędrzejewska-Szczerska, Sensors **17(2)**, 261 (2017).
2. D. Majchrowicz, M. Hirsch, P. Wierzba, M. Bechelany, R. Viter, and M. Jędrzejewska-Szczerska, Sensors **16(3)**, 416 (2016).
3. D. Milewska and K. Karpienko, IOP Conf. Ser. Mater. Sci. Eng. **104(1)**, 12023 (2016).
4. D. Milewska, K. Karpienko and M. Jędrzejewska-Szczerska, Diam. Relat. Mater. **64**, 169–176 (2016).
5. P. Bajaj, D. Akin, A. Gupta, D. Sherman, B. Shi, O. Auciello and R. Bashir, Biomed. Microdevices **9(6)**, 787–794 (2007).
6. M. Amaral, A. G. Dias, P. S. Gomes, M. A. Lopes, R. F. Silva, J. D. Santos and M. H. Fernandes, J. Biomed. Mater. Res. A **87(1),** 91–99 (2008).
7. M. Wąsowicz, M. Ficek, M. S. Wróbel, R. Chakraborty, D. Fixler, P. Wierzba, and M. Jędrzejewska-Szczerska, Materials **10(4)**, 352 (2017).
8. A. V. Sukhadolau, E. V. Ivakin, V. G. Ralchenko, A. V. Khomich, A. V. Vlasov and A. F. Popovich, Diam. Relat. Mater. **14(3)**, 589–593 (2005).
9. G. M. Swain, A. B. Anderson and J. C. Angus, J. C. MRS Bull. **23(9)**, 56–60 (1998).
10. R. Bogdanowicz, Metrol. Meas. Syst. **21(4),** 685-698 (2014).
11. W. Gajewski, P. Achatz, O. A. Williams, K. Haenen, E. Bustarret, M. Stutzmann and J. A. Garrido, Phys. Rev. B **79(4)**, 45206 (2009).
12. G. M. Swain, J. Electrochem. Soc. **141(12)**, 3382–3393 (1994).
13. A. Suzuki, T. A. Ivandini, K. Yoshimi, A. Fujishima, G. Oyama, T. Nakazato, N. Hattori, S. Kitazawa and Y. Einaga, Anal. Chem. **79(22),** 8608–8615 (2007).
14. K. Pecková, J. Musilová and J. Barek, Crit. Rev. Anal. Chem. **39(3)**, 148–172 (2009).
15. P. Niedziałkowski, R. Bogdanowicz, P. Zięba, J. Wysocka, J. Ryl, M. Sobaszek, and T. Ossowski, Electroanalysis **28(1)**, 211–221 (2016).
16. M. Ficek, M. Sobaszek, M. Gnyba, J. Ryl, Ł. Gołuński, M. Smietana, J. Jasiński, P. Caban and R. Bogdanowicz, Appl. Surf. Sci. **387**, 846–856 (2016).
17. M. Sobaszek, Ł. Skowroński, R. Bogdanowicz, K. Siuzdak, A. Cirocka, P. Zięba, M. Gnyba, M. Naparty, Ł. Gołuński and P. Płotka, Opt. Mater. **42**, 24–34 (2015).
18. R. Bogdanowicz, M. Sobaszek, M. Ficek, D. Kopiec, M. Moczała, K. Orłowska, M. Sawczak and T. Gotszalk, Appl. Phys. A **122(4)**, 270 (2016).
19. R. Bogdanowicz, M. Gnyba and P. Wroczyński, J. Phys. IV Proc. **137**, 57–60 (2006).
20. R. Bogdanowicz, M. Gnyba, P. Wroczynski and B. B. Kosmowski, J. Optoelectron. Adv. Mater. **12**(8), 1660–1665 (2010).
21.nova_manual.pdf (http://www.tcelectronic.com/media/218009/tc_electronic_nova_system_manual_english.pdf) (accessed on 01 April 2017).
22. M. Sobaszek, K. Siuzdak, Ł. Skowroński, R. Bogdanowicz and J. Pluciński, IOP Conf. Ser. Mater. Sci. Eng. **104(1)**, 12024 (2016)
23. K. Fabisiak, A. Banaszak, M. Kaczmarski and M. Kozanecki, Opt. Mater. **28(1-2)**, 106–110 (2006)
24. P. K. Chu and L. Liuhe, Mater. Chem. Phys. **96(2-3)**, 253–277 (2006).
25. P. Hariharan, Optical Interferometry (Academic Press: San Diego, 2003), p. 189.
26. K. T. V. Grattan, Optical Fiber Sensor Technology (Kluwer Academic Publisher: Boston, MA, USA, 2000), p. 441